ISSN:2790-1688 DOI: 10.56028/aetr.2.1.368

Microstructure and performance test of aluminum alloy K-TIG welding joint

Weijie Gou*, Lihong Wang

Beijing Polytechnic, Beijing, 100176, china

*Corresponding author's e-mail: gouweijie@bpi.edu.cn

Abstract. The K-TIG welding method was used to conduct welding experiments on 6001 aluminum alloy, and the microstructure and mechanical properties of the welded joints were studied by optical microscope, scanning electron microscope, universal testing machine, microhardness tester, etc. The results show that the center of the weld is equiaxed crystals and a small amount of dendrites, the near seam zone is columnar crystals formed by associated crystals, the fusion zone is equiaxed crystals of varying sizes, and there are grain boundary liquefaction and β″ phase in this zone. Agglomeration, growth and transformation, there are grain growth and precipitation zones in the heat-affected zone; the tensile fracture positions are all at the fusion line, and the fractures are ductile and brittle mixed quasi-cleavage fractures, with dimples, river patterns, and cleavage steps; welded joints The hardness of the fusion zone has a W-shaped distribution, and the hardness value of the fusion zone is lower due to over-aging softening.

Keywords: aluminum alloy; K-TIG welding; microstructure; mechanical properties

1. Introduction

6N01 aluminum alloy has medium strength, good corrosion resistance, workability and weldability. It has been widely used in side walls, roof covers, compartment frames of high-speed trains, subway trains, double-decker trains, passenger and freight cars, etc. [1]. When the traditional welding method of MIG or TIG with low energy density of the heat source is used, due to the high thermal conductivity and linear expansion coefficient of 6N01 aluminum alloy, a large amount of heat has been transferred to the surrounding base material before the workpiece is melted. Heat input causes large welding residual stress, serious softening, and reduced mechanical properties. The heat source energy density of K-TIG welding is high and the arc is concentrated. When the heat input is the same, more heat in the arc is conducted to the inside of the workpiece, which reduces the softening of the welded joint. Therefore, the use of K-TIG welding has the advantages of excellent welding joint quality, high production efficiency, and low cost[2]. At present, research on K-TIG welding is mainly concentrated on low thermal conductivity materials such as stainless steel, titanium and zirconium, and there are few studies on aluminum alloys with high thermal conductivity[3]. Mainly because K-TIG welding is suitable for materials with low thermal conductivity, high surface tension and high liquid metal density. In aluminum alloy K-TIG welding, its higher thermal conductivity will significantly increase the volume of the molten pool and the width of the root of the weld, which will easily lead to instability of the molten pool and collapse or burn through. Therefore, it is of great practical significance to study the structure and properties of 6N01 aluminum alloy K-TIG welded joints.

2. Test equipment, materials and methods

Test equipment: OTC arc welding machine (rated current 500 A) K-TIG welding gun, water-cooled box, weldment mobile control platform. The high-efficiency cooling system of the K-TIG welding gun makes the arc more concentrated and penetrating, enabling high-quality and high-efficiency welding. The supply state of the 6N01 aluminum alloy for the test is T5 (Solid Solution + Artificial Aging), and its structure is composed of α (Al) solid solution and a large number of dispersed and uniformly distributed black granular Mg2Si strengthening phases. The

ISSN:2790-1688 DOI: 10.56028/aetr.2.1.368
grains are distributed along the extrusion direction. And it is fibrous. The microstructure is shown in Figure 1, and the main chemical components are shown in Table 1.

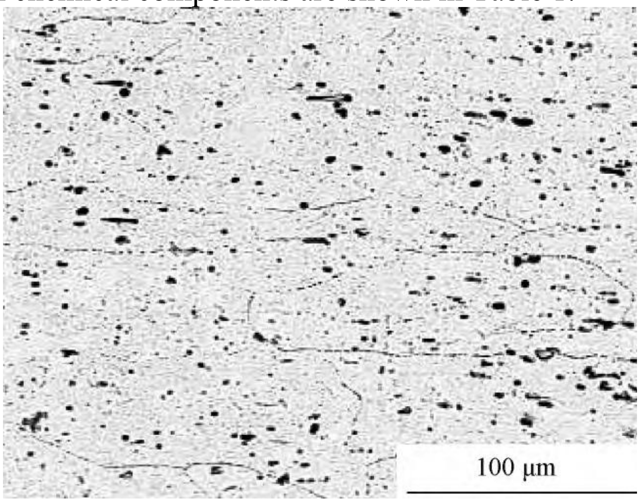

Figure 1. Microstructure of 6N01 aluminum alloy base metal

Table 1. The main chemical composition of 6N01 aluminum alloy (mass fraction) (%)

Si	Mg	Fe	Mn	Cu	Zn	Ti	Cr	Al
0. 65	0. 6	0. 35	0. 5	0. 35	0. 25	0. 1	0. 3	margin

The size of the 6N01 aluminum alloy test plate is 200 mm×100 mm×6mm, with butt joints, no grooves, no filling materials, single-sided welding and double-sided forming technology. Before welding, remove impurities such as oil stains and oxide films on the surface and end faces to prevent defects such as pores and cracks. Because the dense oxide film has high thermal conductivity and large thermal expansion coefficient, it has a high solubility for hydrogen in the molten state, and the bubbles can't escape the surface of the weld during welding and cause more pore defects. At the same time, ensure that the assembly gap is less than or equal to 0.5 mm, and the amount of misalignment is less than or equal to 0.1 mm to complete the tack welding to prevent the size and relative position of the weldment from changing during the welding process. After the tack welding, make the test piece reverse deformation at a small angle Fix it with a jig and prepare for welding; during AC pulse welding, pass a shielding gas to the back of the test piece to improve the cooling rate and oxidation resistance of the liquid metal; after welding, use a DK7725 wire cutting machine to intercept the gold in the direction perpendicular to the welding seam After grinding and polishing the sample, soak the sample in Keller’s reagent (1 mL HF+1. 5 mL HCL+2.5 mL HNO3 + 95 mL H2O) for 60 s, then wipe with alcohol and blow Dry. Use the AxioScope A1 optical microscope to observe the microstructure of the weld, and use the Quanta450 scanning electron microscope to observe the fracture topography. Use the WDW-100D universal testing machine to carry out the tensile test of the welded joint, the loading rate is 2 mm/min, and the loading load is 50kN; the HVS-1000 Vickers hardness tester is used to determine the hardness value of the weld, HAZ and base metal.

3. Test results and discussion

3.1 Macro morphology of welded joints

The macroscopic appearance of the welded joint is shown in Figure 2a, b. The front weld is smooth and flat, the melting width is uniform, the weld pool pattern is uniform and fine, and there is no spatter or undercut. The welding seam on the back is smooth and uniform, and the melting width and the remaining height are uniform. There is no undercut, unfused, and pore defects; the cross-section of the weld is shown in Figure 2c. The liquid metal with small volume and relatively low temperature is distributed at the bottom of the molten pool, causing the liquid metal to form a

ISSN:2790-1688 DOI: 10.56028/aetr.2.1.368

wider upper surface, gradually narrowing in the middle and converging in the middle and lower parts, and the bottom is gradually changing due to the return of the liquid metal after the keyhole is closed. It has a wide "wine glass" shape of the molten pool, and there are no obvious pores and cracks on the surface.

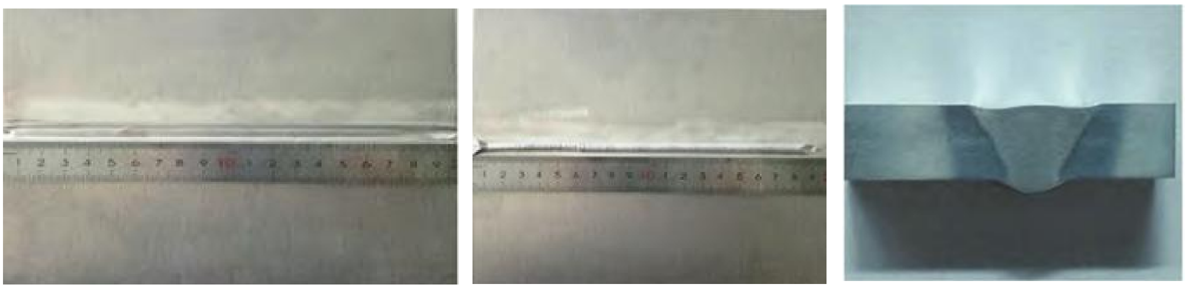

（a）front (b) back (c) cross section

Figure2. Macro morphology of 6N01 aluminum alloy welded joint

3.2 Microstructure of welded joint

The microstructure of the 6N01 aluminum alloy weld zone is shown in Figure 3a, b. The center of the weld is uniform and fine equiaxed crystals and a small amount of dendrites, and columnar crystals are distributed along the heat dissipation direction perpendicular to the fusion line away from the center of the weld. There is a clear dividing line at the intersection of crystal and equiaxed crystal[4]. According to analysis, the Jackson factor α of 6N01 aluminum alloy is less than or equal to 2, and the solid-liquid interface is a rough interface, and there are many places that provide nucleation bases for solute atoms. It is called "Associated Crystallization".

When the liquid metal has a negative temperature gradient at the front of the solid-liquid interface due to a large degree of subcooling, the protrusions that nucleate on the local interface substrate will enter the liquid metal with a greater degree of subcooling and continue to grow due to the latent heat of crystallization. The conduction in front of the tip is faster than that in the lateral direction, resulting in the growth rate of the tip being greater than the lateral growth rate, forming a slender backbone. At the same time, the tip of the polyhedral crystal nucleus that cannot exist stably in the three-dimensional space also grows a dendrite in the direction of easy heat dissipation. As the crystallization process continues, nucleation and growth on the backbone and dendrites will eventually form columnar dendrites; secondly, the columnar crystals produced during the solidification of the molten pool metal will displace some of the unfavorable crystal grains and compete for growth.

Analysis believes that aluminum alloy has a face-centered cubic structure, and its <100> direction is the crystallographic direction that is easiest to grow; on the other hand, when liquid metal is solidified, the protruding tip grows in the normal direction with the fastest heat dissipation. Therefore, when the crystal grains crystallize along the temperature gradient along the direction of maximum heat dissipation in the easiest direction of crystallography, columnar crystals grow fastest and have the largest area, and finally form a coarse columnar crystal structure[5]; Moreover, the center of the weld A larger solidification rate results in a larger crystal growth rate R, while a smaller solidification rate at the fusion line results in a smaller growth rate R. At the same time, because the shape of the weld pool is egg-shaped, the distance from the highest temperature point to the lowest temperature point on the center line of the weld is greater than the distance between the center of the weld and the difference between the high and low temperatures on the fusion line. Therefore, the normal direction of the center line of the weld The temperature gradient above is smaller than that near the fusion line, resulting in G/R at the center of the weld being smaller than the boundary of the fusion line. Therefore, the temperature gradient in the normal direction of the center line of the weld is smaller than that near the fusion line, which ultimately results in the G/R at the center of the weld being smaller than the boundary of the fusion line. Therefore, from the boundary of the fusion line to the center of the weld, as the cooling rate increases, the degree of

ISSN:2790-1688 DOI: 10.56028/aetr.2.1.368
subcooling of the liquid metal component continues to increase, and the solidification mode of the molten pool metal changes from planar growth to columnar crystal growth, and finally waits at the center of the weld. Axial crystal crystallization is over; the structure near the fusion line is shown in Figure 3c, d. The side near the weld is columnar crystals, and the fusion zone is the equiaxed crystal structure of different sizes formed during the recrystallization process; as the heat-affected zone heats up As shown in Figure 3e, the temperature range of β" phase precipitation is 160～240℃, and the temperature range of β' phase precipitation is 240～ At 380℃, due to the difference in the peak temperature of the thermal cycle in the heat-affected zone, the fusion zone produces β" phase segregation, growth, and β" to β'phase transformation.

According to analysis, 6N01 aluminum alloy has a low melting point and weak bonding force between atoms. The higher the aging temperature, the stronger the atom diffusion ability and the faster the precipitation rate. However, as the temperature increases, the strengthening phase in the supersaturated solid solution dissolves to reduce the degree of supersaturation. The difference in free energy between the matrix phase and the desolvent phase and the reduction of lattice distortion result in a decrease in the desolvation rate. The order of the precipitation structure is as follows: supersaturated solid solution→GP→β″(Mg2Si)→β'(Mg2Si), 6N01 aluminum alloy Al, Mg, Si have a small difference in atomic radius (1.43, 1.6, 1. 34)), it is easy to form a spherical GP zone. The formation of the GP zone is related to the vacancy. After the formation of the GP zone, as the aging time increases or the aging temperature rises, Mg and Si atoms are further enriched, grown, and tend to be ordered. When the thermal cycle temperature exceeds 240 ℃, the transition from β” to β'will occur. The formation of β'phase is related to the dislocation density [6]; the partial melting zone of 6N01 aluminum alloy will be welded during welding. Grain boundary liquefaction occurs. Analysis believes that the content of low melting point impurity elements in the grain boundary is relatively high, and it is easy to segregate at the grain boundary and cause liquefaction[7]. The welding heat-affected zone is heated by the thermal cycle temperature to between the eutectic temperature and the liquidus temperature, and the grain boundary melting occurs. After the cooling and crystallization, the gray eutectic and the white bright low-melting aluminum-rich alpha zone distributed along the grain boundary are formed The structure is shown in Figure 3f; when the heat input is large and the cooling rate is slow, the peak temperature exceeds the recrystallization temperature and the high-temperature residence time is longer, resulting in the growth of grains in the heat-affected zone and coarsening. As shown in Figure 3g; when the precipitated phase uniformly nucleates at the grain boundary and within the grain and continuously desolvates, the initial precipitated phase is relatively small. As the granular precipitated phase continues to aggregate and grow, a precipitation zone is formed, which leads to heat The corrosion resistance of the affected area is reduced, and the local area is corroded and blackened [8], as shown in Figure 3h.

ISSN:2790-1688 DOI: 10.56028/aetr.2.1.368

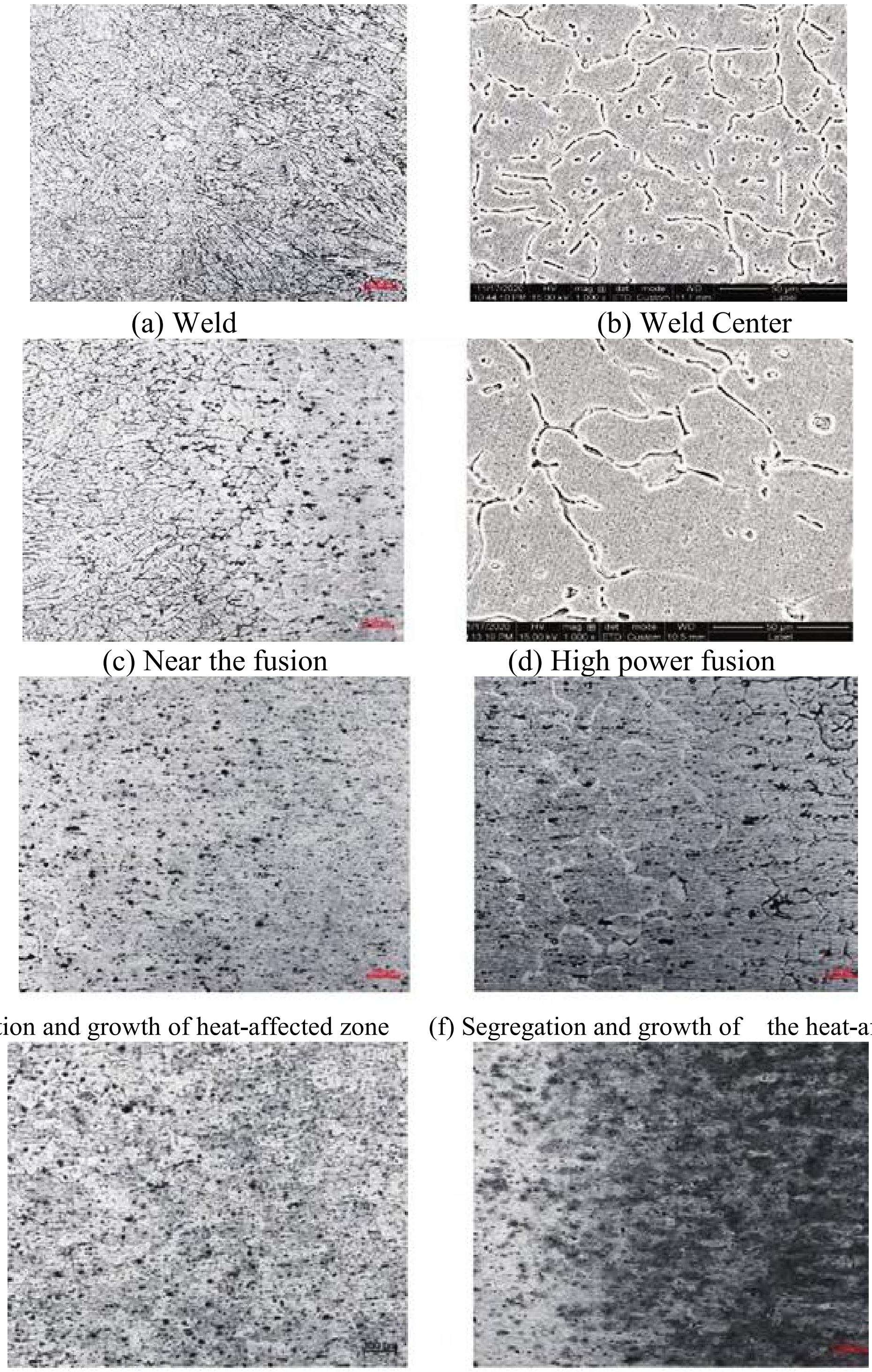

(a) Weld (b) Weld Center

(c) Near the fusion (d) High power fusion

(e) segregation and growth of heat-affected zone (f) Segregation and growth of the heat-affected zone

(g) Grain growth in the heat-affected zone (h)Precipitation zone in the affected zone

Figure 3. Microstructure morphology of 6N01 aluminum alloy welded joint

3.3 Analysis of mechanical properties

3.3.1 Tensile properties of welded joints.

The tensile test at room temperature was performed on the weld specimens. The results are shown in Figure 4. The fractures of the specimens are all at the fusion line, and their tensile strengths are 161 and 167 MPa, respectively, which are in line with the minimum 60% higher than the strength of the base metal. standard requirement. The fusion zone is the weak part of the welded joint. The inhomogeneity of its chemical composition and structure leads to the defects of grain boundary liquefaction, stress concentration, and thermal cracking in the fusion zone, which reduce

ISSN:2790-1688 DOI: 10.56028/aetr.2.1.368
the mechanical properties of the welded joint. According to analysis, in the process of non-equilibrium crystallization of liquid metal, solute atoms diffuse unevenly due to the large degree of subcooling, resulting in a large concentration gradient inside and outside the crystallized solid phase and in the remaining liquid phase, resulting in a large concentration gradient within and between phases. Segregation occurs due to uneven composition, which seriously affects the structure and performance of the weld. At the same time, the decrease in strength is also related to the recovery of the GP zone formed during natural aging. The higher the temperature in the heat-affected zone, the faster the natural aging will proceed, and the more obvious the decrease in strength will be.

(a)Front side (b) Back side

Figure 4. Breaking position of tensile specimen of welded joint

The scanned photograph of the tensile fracture of the welded joint is shown in Figure 5. The fracture changes from ductile fracture to brittle fracture, and the fracture is a mixed fracture of ductility and brittleness. The dimples are distributed deeper and larger in size, as shown in Figure 5a, and the tearing edge formed during the plastic deformation process is shown in Figure 5b. The brittle fracture part has quasi-cleavage characteristics, with obvious river patterns and cleavage steps [9], as shown in Figure 5c, d. The EDS scan of the tensile fracture is shown in Figure 6. After the pulse K-TIG welding thermal cycle, a large number of small-sized granular (AlFeSi) precipitates are formed at the bottom of the fracture surface. This ductile-brittle mixed fracture behavior It is related to the distribution, size and volume fraction of the precipitated phases.

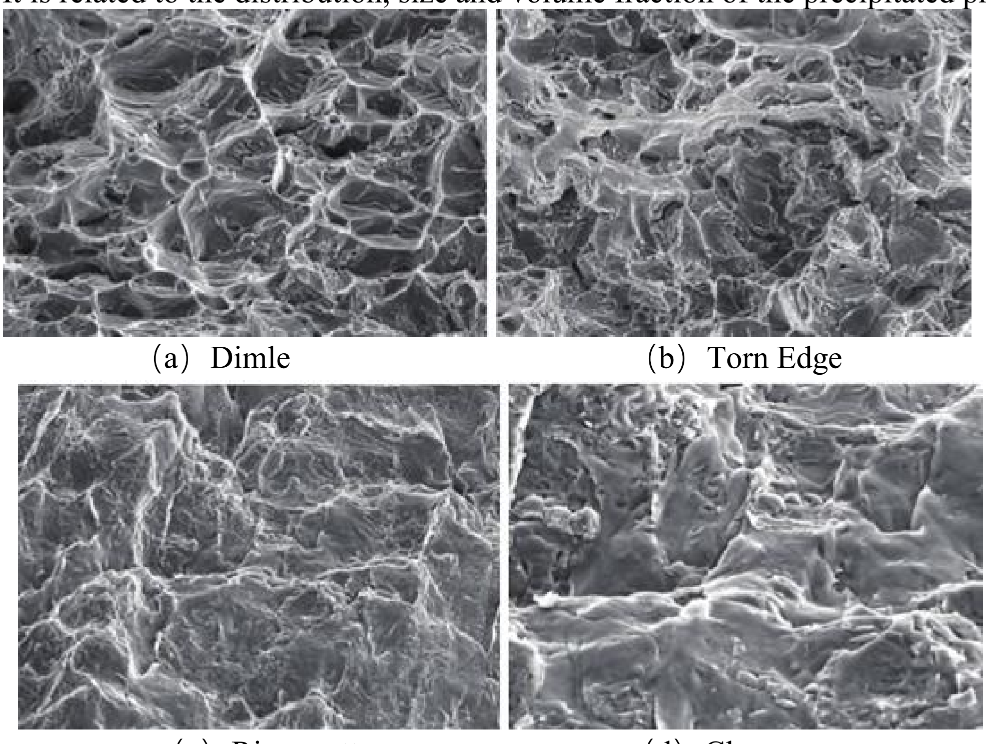

（a） Dimle （b） Torn Edge

（c） River pattern （d） Clesvage

Figure 5. Tensile fracture morphology of welded joint

ISSN:2790-1688 DOI: 10.56028/aetr.2.1.368

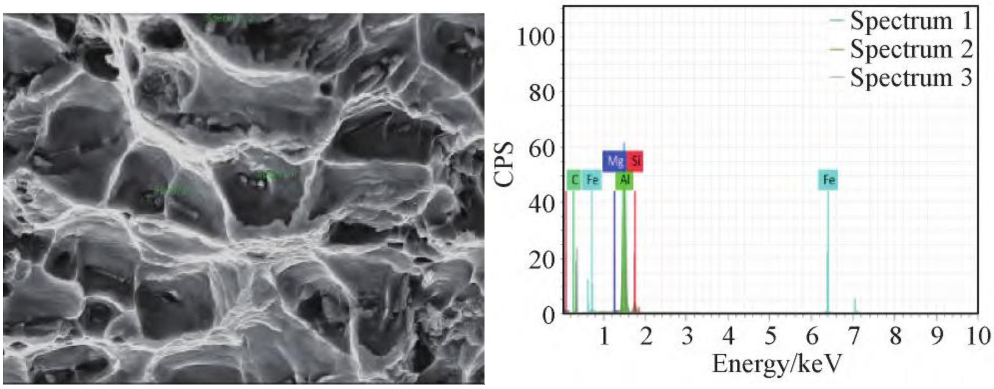

Figure 6. EDS scan of tensile fracture of welded joint

3.3.2 Joint hardness analysis.

As the microstructure and structure change during the desolvation and aging process, the hardness will also change significantly. The microhardness of the weld, the heat-affected zone, and the base metal was measured in the horizontal direction at the center line of the cross section (the measuring point interval is 0.3 mm), and the hardness distribution is shown in Figure7.

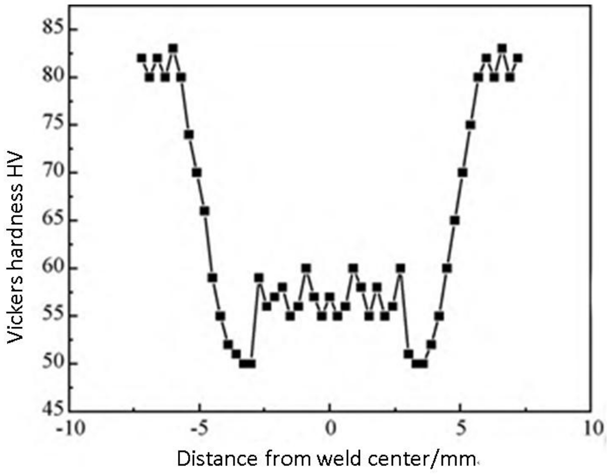

Figure 7. Hardness distribution of 6N01 aluminum alloy welded joint

It can be seen from Fig. 7 that the hardness of the welded joint is approximately symmetrically distributed with the centerline of the weld as the axis. The hardness of the center of the weld is relatively low, and its value is about HV55～HV60; the hardness of the fusion zone at a distance of 3 to 5 mm from the center of the weld is the lowest, and its value is HV50; as the distance from the center of the weld increases, its hardness Gradually increase, and finally reach the hardness of the base material. Analysis shows that β″ phase has a strong strengthening effect, and its precipitation temperature range is 160-240 ℃, while β'phase strengthening effect is weak, and its precipitation precipitation temperature range is 240-380 ℃. As the heat-affected zone heats up With the increase of the cycle temperature, the β" phase aggregates and grows after precipitation and transforms into the β'phase, which leads to the destruction of the coherent relationship in the fusion zone, resulting in over-aging softening, and reduced strength and hardness [10]. At the same time, due to the evaporation and loss of Mg in the weld metal during the high temperature welding process, the Mg in the partial fusion zone migrates to the magnesium-poor weld metal, resulting in a decrease in the hardness of the area.

4. Conclusion

6N01 aluminum alloy test plate with a thickness of 6 mm, no grooves, no gaps, no filling materials, through the K-TIG welding method can achieve single-sided welding and double-sided

ISSN:2790-1688 DOI: 10.56028/aetr.2.1.368
forming and good quality of the welded joint; the center of the weld is Equiaxed crystals and a small amount of dendrites, the near-slit zone is columnar crystals formed by associated crystals, the fusion zone is equiaxed crystals of different sizes, and there are grain boundary liquefaction and β″ phase aggregation, growth and transformation in the fusion zone. There are grain growth and precipitation zones in the affected zone.

The tensile samples are all broken in the fusion zone, and the tensile strength of the weld is about 164 MPa, which meets the requirements of the standard. The tensile fracture is ductile and brittle quasi-cleavage fracture; the joint hardness is W-shaped distribution, the hardness of the weld center is about HV57, and the hardness of the fusion zone is reduced due to overaging softening, and its value is about HV50.

Acknowledgments

This work was financially supported by Beijing Polytechinc Research fund.

References

[1] Peng J., Zhou S, Zhang D.F.(2010) Microstructure and properties of 6N01 aluminum alloy welded joints for high-speed trains.Heat Treatment of Metals, 11: 33-36.

[2] Port P L, Laugier M, Scandella F, et al. (2007)K-GTAW process: A new welding technology combining quality and productivity.Welding International, 216: 430-441

[3] Cui S, Shi Y, Sun K, et al. (2018)Microstructure evolution and mechanical properties of keyhole deep penetration TIG welds of S32101 duplex stainless steel.Materials Science and Engineering: A,709: 214-222.

[4] Wang Y.P, Qin B.J, Chang B.Q et al. (2018)Keyhole welding of AA2219 aluminum alloy with double-pulsed variable polarity gas tungsten arc welding.Journal of Manufacturing Processes, 348:179-186.

[5] Wei J.(2015)Research on the microstructure and properties of 6082-T6 aluminum alloy pulse laser welding joint. Jilin UniversityPh.D. thesis ,pp.103-119.

[6] Zhou W.b, Tan S, Xie S.S, etc. (2014)Aging precipitation behavior of 7N01 aluminum alloy and its effect on properties.Light Alloy Processing Technology, 424: 60-64.

[7] Jin W.F, Shen Q.M, Wei P.Y, et al. (2019)Research on welding technology of 6061-T6 A356-T6 aluminum alloy. Nonferrous Metal Processing, 486: 24-26.

[8] Liang Z.M, Shi K.N, Li W.P, et al. (2018)Microstructure and properties of 6N01 aluminum alloy water-cooled MIG welded joint. Transactions of the China Welding Institution, 399: 25-30.

[9] Li X.Y, Wang X.P, Lei Z, et al.(2015) Analysis of the softening behavior of the laser hybrid welding joint of the 6N01 side wall of the high-speed train.Transactions of the China Welding Institution, 366: 95-98.

[10] Wang Y J, Wei B, Guo Y Y, et al.(2017) Microstructure and mechanical properties of the joint of 6061 aluminum alloy by plasma-MIG hybrid welding.China Welding,2: 58-64.